

X-ray emission of the shock of SN1006.

Constraints on electron kinetics

O.Petruk¹, F.Bocchino², G.Castelletti³, G.Dubner³, D.Iakubovskiy⁴, M.Kirsch⁵, M.Miceli², I.Telezhinsky⁶

¹Institute for Applied Problems in Mechanics and Mathematics & Astronomical Observatory (Lviv, Ukraine)

²INAF-Osservatorio Astronomico di Palermo & Consorzio COMETA (Italy)

³Instituto de Astronomia y Física del Espacio (Buenos Aires, Argentina)

⁴Institute for Theoretical Physics (Kiev, Ukraine)

⁵European Space Astronomy Centre (Madrid, Spain)

⁶Astronomical Observatory in National University (Kiev, Ukraine)

SNRs and kinetics of electrons

Supernova remnants (SNRs) are believed to be the main sources of galactic cosmic rays. The discovery of the nonthermal X-ray emission from the shell SNR SN 1006 (Koyama et al., 1995), the a new way of studies – theoretical and experimental – on galactic cosmic rays, acceleration processes and nonthermal emission of strong nonrelativistic shocks.

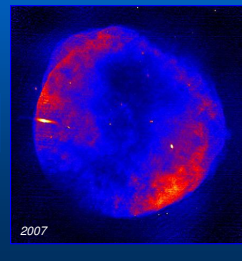
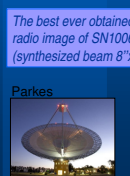
The X-ray spectrum of a region of SNR close to the shock is the most informative one. It is in general a mixture of (at least) two components: thermal and nonthermal emission. There are two key parameters which allow to separate these components: the level of electron ion equilibration χ_s , and the electron injection efficiency ζ .

The thermal X-ray spectrum is sensitive to the post-shock electron temperature T_e , while hydrodynamic deals with the mean post-shock temperature of the plasma T_p . The level of electron ion equilibration defined as $\chi_s = T_e/T_p$ matches experimental data to theoretical model. The theoretically possible range is from $\chi_s = 10^{-3}$ in case of no equilibration to $\chi_s = 1$ in case of full equilibration. Experimental estimation remains

The goal of the present study is to trace the behaviour of the electron-ion equilibration level χ_s , the electron injection efficiency ζ , maximum energy of accelerated electrons E_{\max} over the strong nonradiative shock in SNR.

For this purpose, the radio and X-ray observations of SN1006 are used. These are the archive X-ray data from XMM-Newton observatory as well as newly processed Parkes and VLA radio observations including the data in AB configuration of VLA which provides highest angular resolution.

Radio observations

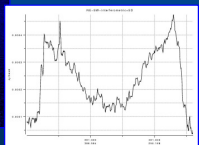


The image at 230 cm was produced on the basis of archival VLA data obtained in October 1991, February 1992 and July 1992 in the hybrid AB, BC and CD configurations, respectively. The observations in the AB configuration were carried out at 1370 and 1376 MHz, while the observations in the BC and CD arrays were performed at 1370 and 1605 MHz. The data corresponding to the more compact configurations of the VLA, BC and CD, were published in a part of the experimental study of SN 1006 (Morfill et al., 1993). The observation performed with the more extended structure array AB, which provide the highest angular resolution, however, were never processed.

The new measurements image structure with angular scales from all spatial structures with angular scales larger than 15 arcsec and 15 arcmin. To recover the density distribution from structures on angular scales larger than 15 arcmin which is important in this case since SN1006 is "30 arcmin in diameter" we added single dish observations acquired in 2002 with the Parkes dish in radio telescope. The image has a synthesized beam of $7.7'' \times 4.8''$, position angle 8° , an rms noise of 1.1 mJy/beam , and the total recovered flux is 1.14 Jy .

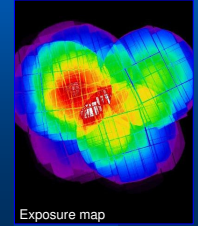
We make use of:

- Brightness profiles
- Fluxes for X-ray analysis
- Detailed map for comparison with X-ray images



X-ray observations with XMM

SN1006 was observed by XMM 8 times in period 2000-2005. Total cleaned exposure is 122 ksec

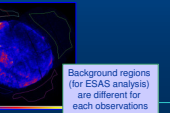


Two different methods are used for analysis of X-ray spectra

In the first approach, we use the Extended Source Analysis software package (XMM-ESAS) for analysis of a set of observations from the EPIC-MOS camera.

We have prepared a procedure which is similar to the "double background subtraction" technique (Read & Proust, 2003). In this procedure, the instrumental background is subtracted applying the method of Saunders & Katz (2008), with the use of data from the unexposed sky corner of the EPIC-MOS detectors; then the cosmic background is modelled. To model the cosmic and soft proton background, we choose the background regions, close to the SN1006 (Fig. 1), and model the obtained "cosmic background" spectra in XSPEC. After receding of model components, we subtract the obtained background model into source regions.

In the second approach we use the Science Analysis System (SAS). We derive the contribution of the background from high signal-to-noise blank fields and we subtract it taking into account the subregion geometry of the instrument across the field of view. The fittings were performed simultaneously on both MOS and pn-cam spectra.

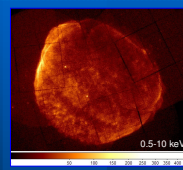


The spectra from source regions are modelled using XSPEC and considering a thermal VSPHOCK component with variable abundances of Fe, Ni, Si, plus a non-thermal SEXT component with two free parameters (i.e. spectral index, α , and break, E_b , the normalization being derived from the ratio data/fit). Since the non-thermal levels of SN 1006 is difficult to compare the parameters of the thermal component, for each limit we chosen these parameters to the mean values obtained in the adjacent thermal regions (where they are quite uniform). We also an assumption between the best fit values of α and β in the thermal regions, which we solved using the α value derived in adjacent non-thermal regions (where it is quite uniform).

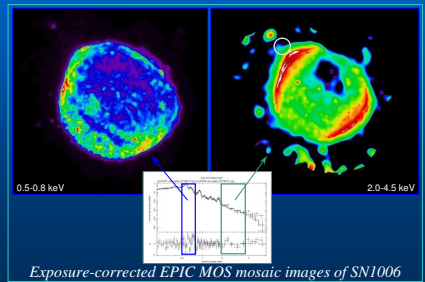
This allow us to obtain relatively low values of the reduced χ^2 ($\chi^2_{\text{red}} \sim 1.2$) and robust results across the shock rim.

Results of the spectral fitting in these two approaches are compared. In both approaches, parameters characterizing thermal and nonthermal components in the X-ray spectra are quite close in each source region.

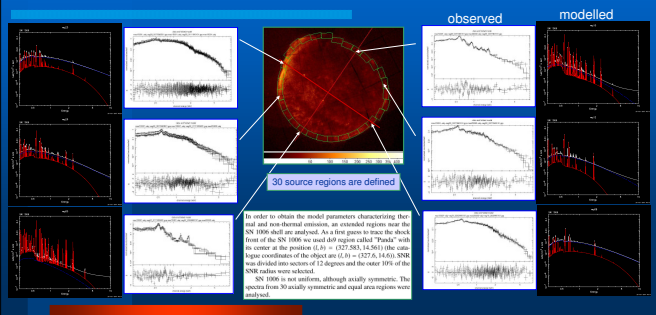
X-ray mosaic images



After removing non-filter, additional exclusion of soft proton flaring periods from the event files with the help of zero-flux, event on is done. This produced cleaned MOS images which used to obtain the mosaic image (with SAS tool). The mosaic image is further smoothed and exposure corrected. The reason for that is to determine the goodness of spectra, produced from selected regions, which is proportional to count number rather than event rate.



Source regions and spectra



In order to obtain the model parameters characterizing thermal and non-thermal emission, an extended region near the SN 1006 shell are analysed. As a first guess to trace the shock front of the SN 1006 we used 409 region called "Parks" with its corner at the position (J2000) (127.65, 14.56) (the coordinate of the object are (J2000) (127.6, 14.6)). SNR was divided into sectors of 12 regions and the outer 10% of the SNR values were selected.

SN 1006 is not uniform, although axially symmetric. The spectra from 30 axially symmetric and equal area regions were analysed.

Parameters of interest

The goal is to estimate:

- electron thermalization level χ_s ,
- electron injection efficiency ζ ,
- energy partition between thermal and nonthermal electrons $E_{\text{nth}}/E_{\text{th}}$,
- maximum energy of accelerated electrons E_{\max}
- their dependence on the shock velocity V and
- on the shock obliquity

Observations yield:

$$T_{\text{es}}, n_{\text{es}}, R, F_s, s, V_{\text{max}}$$

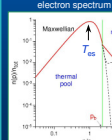
Level of electron thermalization

$$\chi_s = T_{\text{es}}/T_s$$

$$T_s = \frac{\sigma - 1}{\sigma + 1} \frac{\mu m_e V^2}{k_B}$$

$$V = \frac{2}{5} \left(\frac{E_{\text{es}}}{\sigma \mu m_e R} \right)^{1/2} R^{-1/2}$$

$$\chi_s = \frac{25 \sigma \mu m_e R^3}{4 \mu (\sigma - 1)} T_{\text{es}} n_{\text{es}} R^3$$



Injection efficiency of electrons

The spectrum flux of relativistic electrons at some radio frequency ν is $F_\nu = \nu^{-\alpha} N_{\text{es}} d^2$ where N_{es} is the volume of emitting region, d is the distance to SNR, $F_\nu = C_{\text{es}} R^2 \nu^{-\alpha}$ is the emitting C_{es} for the known constant. Thus, for our regions

$$F_s = \frac{C_{\text{es}}}{4\pi d^2} \nu^{-\alpha} R^2 \nu^{-\alpha} \quad (7)$$

$$\zeta = \frac{\sigma - 1}{\sigma + 1} \frac{\mu m_e V^2}{k_B} \frac{F_s}{F_{\text{th}}} \quad (8)$$

The break momentum p_b is the momentum where Maxwellian electron distribution matches the nonthermal power-law distribution of accelerated electrons is

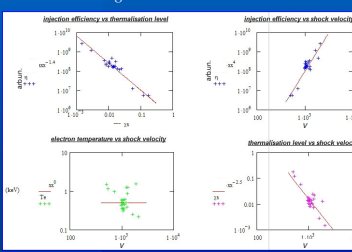
$$p_b = 3.5 p_{\text{th}} = \frac{\sigma^{1/2} T_{\text{es}}}{V} \quad (9)$$

It is important to note that the coefficient μ/p_b is 3.7 able to change in 10-20% only for wide range of $\sigma = 10^3 - 10^5$. Substituting (9) with (9) and E_{th} from (9) gives

$$\zeta = \frac{4 \mu (\sigma - 1)}{C_{\text{es}} R^2 \nu^{-\alpha}} \frac{F_s}{F_{\text{th}}} \quad (10)$$

Thermal and nonthermal electrons

in the source regions around the shock in SN1006



Trends (preliminary)

- $\zeta \propto \chi_s^{-1.4}$
- $\zeta \propto V^4$
- T_{es} does not reveal any dependence on V
- $\chi_s \propto V^{-2.5}$
- $E_{\text{nth}}/E_{\text{th}} \propto V^{4.5}$
- E_{\max} is limited by the age of SN1006

Conclusions

Electrons around the shock in SN1006 reveal the following properties (preliminary results)

E_{\max} is within 20-60 TeV
 E_{\max} is limited by the age of SN1006, not by the radiative losses

The higher electron-proton equilibration the smaller injection efficiency: $\zeta \propto \chi_s^{-1.4}$, in agreement with model of Petruk & Bandiera (2006).

T_{es} does not reveal any dependence on the shock velocity V , in agreement with model of Ghavamian et al. (2007).

Since $T_{\text{es}} \propto V^2$ then the expected dependence of thermalization level on V is $\chi_s \propto V^{-2}$. This is close to our preliminary trend $\chi_s \propto V^{-2.5}$

$E_{\text{nth}}/E_{\text{th}}$ increases with V , due to decrease of the electron thermalisation level and increase of the electron injection efficiency